Theoretical and experimental study of supersonic gas jet targets for laser wakefield acceleration

Fabio B. D. Tabacow
IPEN – CNEN/SP
São Paulo, SP, Brazil
fabio.tabacow@gmail.com

Armando V. F. Zuffi
IPEN – CNEN/SP
São Paulo, SP, Brazil
armandozuffi@gmail.com

Edison P. Maldonado
Instituto Tecnológico de Aeronáutica
São José dos Campos, SP, Brazil
puig@ita.br

Ricardo E. Samad
IPEN – CNEN/SP
São Paulo, SP, Brazil
resamad@gmail.com

Nilson D. Vieira Jr.
IPEN – CNEN/SP
São Paulo, SP, Brazil
nilsondiasvieirajr@gmail.com

2021 SBFoton International Optics and Photonics Conference (SBFoton IOPC) | 978-1-6654-1948-2/21/$31.00 ©2021 IEEE | DOI: 10.1109/SBFOTONIOPC50774.2021.9461936

Abstract—This work reports a theoretical and experimental study of supersonic gas jets to be used as targets in laser wakefield acceleration. A comparison between theoretical and experimental results ismade in order to estimate the results of a de Laval nozzle manufactured in our laboratory, used to produce a N_2 gas target. The comparison between the results shows that Computational Fluid Dynamicssimulations are able todescribe the phenomena of the supersonic gas jet.

Keywords—de Laval nozzles, CFD simulation, interferometry, gas density, laser wakefield acceleration

I. INTRODUCTION

The use of laser wakefield acceleration systems (LWFA) has grown rapidly in the scientific community as a newtechnology for particle accelerator systems [1, 2]. This technique relies on the generation of acceleration gradients above 100 GV/m, which are currently limited to the order of 100 MV/m [3] in conventional RF accelerators due to materials breakdown. It also reduces the size and complexity, and consequently the costs, of particle accelerators. Moreover in this type of acceleration systems, usually renewable and fluid targets are used create the plasma and stimulate the generation of a longitudinal electric field (wakefield) capable of accelerating electrons [4]. The interaction of particles (electrons) with matter allows the development of compact and tunable sources, which can be used in many applications asnew imaging techniques [5] and production of medicinal radiocompounds[3, 6, 7].

Usually, lasers with peak powers ranging from TW to PW are used to accelerate electrons [8, 9], but recent advances were obtained in the acceleration with sub-TW pulses [10-12].To achieve acceleration with these lower powers, gas jets targets with ~100 µm thickness and densities between 10^{18} and 10^{21} atoms/cm³ are needed to ensure that Self-Modulated Laser Wakefield Acceleration (SM-LWFA) [8, 13, 14] occurs, and generate highly nonlinear waves of plasma even for mJ-class laser pulses [7].Gas targets in the form of supersonic jets are necessary to provide new, reproducible conditions fast as possible to each laser pulse.

De Laval nozzles [15, 16] are convergent-divergent nozzles used to accelerate fluids to supersonic speeds (high Mach numbers). With this kind of nozzle, sharpjet-vacuum boundaries are created and homogeneous flat-top gas density profiles are typically obtained. These characteristics can simplify the design and control of laser-plasma experiments by enhancing the laser interaction with the fluid [17].

High-intensity laser experiments currently using de Laval nozzles involve laser frequency upshift and high-harmonic generation, laser filamentation, relativistic self-focusing, laser-driven electron acceleration, THz generation, extreme ultraviolet and x-ray beam generation, laser pulse compression, among others [8].Infrastructures [17, 18]are being prepared to produce particle beams to be used in medical applications like x-ray and electron therapy, nuclear reactions and, eventually, protontherapy [18].

We are workingto implement LWFA in our laboratory, which demands the use of gas jet laser targets to accelerate electrons. Those targetsare being generated by homemade nozzles and compared totheoretical analysis made by Computational Fluid Dynamic (CFD) simulations, with a Finite Element Method (FEM) in the Ansys software, version 19, Academic. Supersonic gas jets are generated, and their experimental analysesare made by interferometer and Schlieren images and compared to the theoretical results to provide feedback to improve the nozzles and targets.

De Laval nozzles [15, 19]are designed to generate supersonic gas jets, by constricting the flow in a throat and then allowing its free expansion. A scheme of a typical de Laval nozzle is represented in Fig. 1, where P_0, T_0, ρ_0 and P_1, T_1, ρ_1 are the pressure, temperature, and density for the backing and experimental chambers, respectively, r_t is the throat radius and r_e is the radius of the nozzle exit.

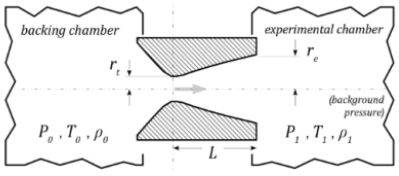

Fig.1. Sketch of a typical de Laval nozzle [20].

A simple quasi-1D [21] model can estimate the gas jet Mach number$M$ based only on the ratio of the exit and throat areas, A_e and A_t, respectively, and the type of gas used:

$$\frac{A_e}{A_t} = \frac{1}{M}\left[\frac{2+(\gamma-1)M^2}{\gamma+1}\right]^{\frac{\gamma+1}{2(\gamma-1)}}, \quad (1)$$

where γ is the is the gas heat capacity ratio, or adiabatic index. This relation gives a starting point to design nozzles with a desired Mach number, providing the sizes of the nozzle throat and exit. As an example, Fig. 2 presents eq. (1) graphically, depicting the ratio of the nozzle throat and exit areas as a function of the Mach number for nitrogen gas.

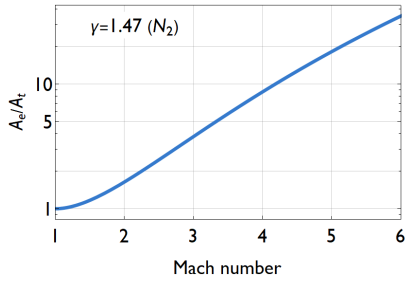

Fig. 2. Dependence of the exit and throat areas ratio on the Mach number for N_2.

This quasi-1D model disregards the exact value of the background pressure into which the jet expands, the presence of shock waves, as well as the nozzle length and other geometrical features like the length of the converging region, shapes and curvatures, all these affecting the jet discharge and speed (and pressure) as second-order corrections. To better understand and design nozzles, more sophisticated models or numerical simulations, such as the one used in this work are needed.

II. Methodology

We assembled a Mach-Zehnder interferometer with Schlieren imaging, shown in Fig. 3, to characterize the profile and density of the gas jets generated by the homemade de Laval nozzles. A polarized green HeNe CW beam is spatially filtered by a pinhole and collimated to a 1 cm radius beam. This beam is split in a Mach-Zehnder interferometer, and one of its armscontains the gas jet. After the beamsexit the Mach-Zehnder, a 10 cm converging lens is positioned in the final of optical axis and 12 cm away from the jet, projecting a 5× magnified image of the jet in a CCD surface. A knife-edge is positioned on the lens focus to produce a Schlieren image in the same CCD, when blocking the beam in the arm without the jet.Furthermore, we have manufactured a small vacuum chamber [20], with Brewster windows, which can be fitted to the nozzle. The jet can be characterized either in atmosphere orinside the small vacuum chamber when applying a nitrogen backing pressure up to 50 bar. At this high backing pressure, the residual pressure inside the chamber is ~20 mbar.

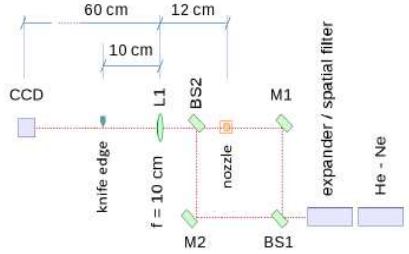

Fig. 3. Setup for measurement of the gas jet through Mach-Zehnder interferometer and Schlieren images.

The phase-shift caused by the gas jet is made visible by the bending of the fringes in the interferogram [22]. Optical path differences due to gas density variations result in deformations of the fringes, to which the phase-shift is proportional.

The Computational Fluid Dynamic (CFD) simulations were used as a tool to understand the flow and all phenomena that can happen when a gas is forced through a home-made de Laval nozzle. The simulated nozzle was etched in a 600 µm thickalumina (Al_2O_3) plate by anultrashort pulse machining system in our lab. Its exit and throat diametersare 190 µm and 86 µm, respectively, defining a Mach number of ~3to nitrogen gas, according to the graph shown inFig. 2.

The fluid simulated in this work is ideal N_2, with a CFX module from Ansys 19, Academic version, and the gas flow is described by the Navier-Stokes differential equations, which are solved using the upwind scheme discretization method. The turbulence is modeled by the K-ε method, which uses two equations based on the turbulent viscosity concept. This parameter of viscosity inside the flow is an unknown term that needs to be modeled numerically. This viscosity may be written as a function of K and ε, which are, respectively,the turbulent kineticenergy and the viscosity dissipation of this energy. The backing pressure is 50 bar and the background pressure is determined with the exhaust pressure of 20mbar.

III. Results

A. Experimental Analysis

Fig. 4shows an interferogram of the Mach 3 manufactured nozzle [20], using N_2 with a backing pressure of 50 bar. The interferogramwas measured inside the vacuum chamber,with 20 mbar of background pressure. The red rectangle shows the fringes deformation, indicating theregion with the gas jet axis.

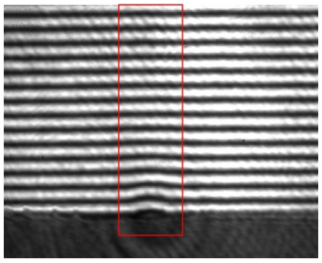

Fig. 4. Image for interferometer Mach-Zehnder of a gas jet (N_2) flowing through a de Laval nozzle in vacuum (20 mbar background pressure).

Fig. 5.a) presents the phase-shift map obtained from the interferogram shown in Fig. 4, and the corresponding density map, (b), derived from it considering the gas refractive index induced phase-shift:

$$n = 1 + \Delta\phi\,\lambda/(2\pi l), \quad (2)$$

where $\Delta\phi$ is the measured phase-shift, $\lambda = 543$ nm is the interferometer laser wavelength, and l is the gas jet diameter, which was estimated from the phase map to be 190 µm assuming a cylindrical symmetry of the jet and a background refractive index of 1 (ideal vacuum). From the refractive index 2D map and eq. (2) we also can estimate the gas density distribution using the simple expressionof the Lorentz-Lorenz relation [23, 24]:

$$\rho = 3/(4\pi\alpha)\times(n^2 - 1)/(n^2 + 2), \quad (3)$$

where α is the molecular polarizability, which for N_2 is 1.710 $Å^3$ [25].

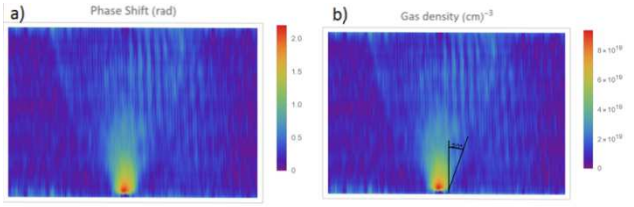

Fig. 5. a) Phase-shift map of a gas jet flowing from the De Laval Nozzle. b) Gas density map obtained by the phase-shift map.

From the density map we can see that the jet divergence angle is ~20°. The simplified quasi 1-D model provides a simple expression, [21] to estimate the relation between the jet Mach number, *M*, and its divergence, α:

$$\alpha = 1/M, \quad (4)$$

and from this equation we can estimate $M \approx 2.8$.

B. Theoretical Analysis

The de Laval nozzle that was simulated has a conical geometry, with cylindrical transversal section. Its exit diameter is 190µm and the throat diameter is 86 µm,with the length of the nozzle being 600 µm, with low roughness walls. Those dimensions are the same that the nozzle used in our experiments.Fig. 6shows the Mach (speed) distribution of the gas jet flow through the de Laval nozzle and after its exit. It can be easily seen that the maximum speed occurs near the nozzle exit, with a Mach number of ~2.5. The discrepancy between this Mach number and the value of 3 obtained from Fig. 2comes from the simplified 1D model that provides the curve shown, which disregards the nozzle length and shape, and also the 20 mbar background pressure.

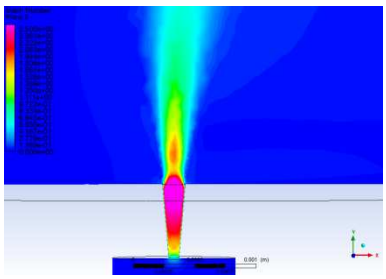

Fig.6. Mach number distribution of the gas jet flowing through the de Laval nozzle and exiting into the vacuum chamber. The Mach number distribution is represented by a color map.

Fig. 7, Fig. 8 and Fig. 9 show the moleculesdensity distributionon the gas jet in different planes. From these pictures, the cylindrical symmetry of the jet can be seen, and it is also possible to verify the sharp transversal density increase in the target, characteristics that are desired for the LFWA. The density decreases along the nozzle as the gas jet velocity grows, reaching a minimum value at the exit, then increasing again

The inhomogeneitiesin Fig. 7, Fig. 8 and Fig. 9are simulation artifacts arising due to non-ideal discretization of the space,arising from restrictions on the grid due to the academic license (limitation on the maximum number of nodes and elements of the grid) that result in a simulation that does not describe the physical system adequately.Because of the relatively small number of space elements allowed, it is necessary to decrease the simulation volume, while keeping it large enough to minimize interferences of the volume walls in the flow. The number of mesh elements influences the spatial resolution of the simulation. Another consequence of the finite volume of the vacuum chamber is the residual background pressure. An exhaustion duct was created to extract the gas from the simulation volume, but the flow is not enough to keep a low vacuum, resulting in a background pressure that limits the gas expansion.These simulation limitations are responsible for the discrepancies between the simulations and the results experimental results, and studies are being done in order to further reduce the background pressure and improve the simulation volume discretization, thus bringing the theoretical results closer to the experimental ones.

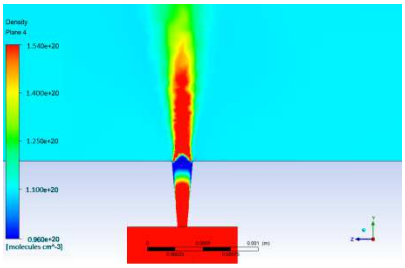

Fig. 7. Density distribution in ZY plane of the gas jet flowing through the De Laval nozzle and exiting into the vacuum chamber.

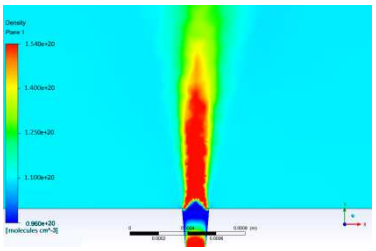

Fig.8. Density distribution in XY plane of the gas jet flowing through the de Laval nozzle and exiting into the vacuum chamber.

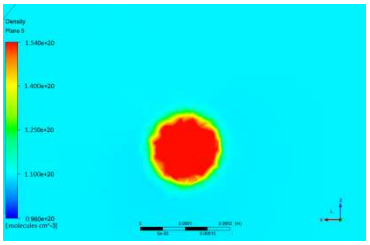

Fig.9. Density distribution in XZ of the gas jet flowing through the de Laval nozzle at the entrance of the vacuum chamber.

C. Comparison between theory and experiments

It is possible to verify that the simulations describe the geometry ofthe gas jet closely to the experimental results, mainly the obtained Mach number and density close to the nozzle exit orifice [21],although the experimental jet is more divergent than the theoretical prediction. In Fig. 7 and Fig. 8is possible to see a region with a great density variation near the nozzle exit. There are also other discrepancies when comparing results, like the jet Mach number determined from the interferograms, which is 2.8 while the maximum Mach from the simulation is 2.5. This difference is due to

the simplified model [21] used in the experimental data, which disregards the nozzle length and background pressure. Despite these differences, the simulation provides a good estimate from a simple model. For the density distributions shown in figures 5b, 8 and 9, there is a difference by a factor 2 since the peak experimental density is ~9×10^{19} molecules/cm^3, while the theoretical peak density reaches and ~1.5×10^{20} molecules/cm^3. This value discrepancy probably arises from considering the gas density constant along the laser path in the interferogram. A more realistic density estimate would need to recover the gas transversal profile considering a cylindrical symmetry, which would increase the experimental retrieved peak density by a factor 2-3. This retrieval can be done by an Abel transform [26, 27], and we are working to implement this technique.With all these considerations, the experimental and theoretical results are close, indicating that the numerical simulations are representing the real phenomena.

IV. Conclusions

In this work, we presented the results of numerical simulations that describe experimental results of gas jet flows fairly close. Theprediction obtained from the simulations can simplify the process of creating different gas target geometries from the design of the de Laval nozzles.

We are working to improve our simulations, and increase their resolution, aiming to get more realistic results that will allow the design of better nozzles and gas targets, optimized for electron acceleration with our laser.

With the knowledge that we are acquiring in this study, it will be possible to perform simulations of more complex systems, like asymmetrical nozzles [28], which produce more complex gas distributions that can improve the electron acceleration process, andsimulate other mixtures of gases that also enhance the acceleration, contributing to our experimental developments.

Acknowledgment

The authors would like to acknowledge the financial support from FAPESP, CNPq and SAE, and a CNPq scholarships toZuffiand Tabacow.

References

[1] T. Katsouleas, "Accelerator physics - Electrons hang ten on laser wake," Nature, vol. 431, pp. 515-516, 2004.

[2] T. Tajima, K. Nakajima, and G. Mourou, "Laser acceleration," Riv. Nuovo Cimento, vol 40, pp. 33-U102, 2017.

[3] A. Giulietti, "Laser-Driven Particle Acceleration Towards Radiobiology and Medicine", Springer International Publishing, 2016, pp.

[4] E. Esarey, C. B. Schroeder, and W. P. Leemans, "Physics of laser-driven plasma-based electron accelerators," Rev. Mod. Phys., vol 81, pp. 1229-1285, 2009.

[5] F. Albert, "Laser Wakefield Accelerators: Next-Generation Light Sources," Optics and Photonics News,vol 29(January 2018), pp. 42-49, 2018.

[6] K. Nemoto, "Laser-triggered ion acceleration and table top isotope production," Appl. Phys. Lett.,vol 78, pp. 595-597, 2001.

[7] I. Spencer, "Laser generation of proton beams for the production of short-lived positron emitting radioisotopes," Nucl. Instrum. Meth. B, vol 183, pp. 449-458, 2001.

[8] J. Faure, "A review of recent progress on laser-plasma acceleration at kHz repetition rate," Plasma Phys. Contr. Fus.,vol 61, pp., 2019.

[9] S. M. Hooker, "Developments in laser-driven plasma accelerators," Nat. Photonics,vol 7, pp. 775-782, 2013.

[10] A. J. Goers, "Multi-MeV Electron Acceleration by Subterawatt Laser Pulses," Phys. Rev. Lett.,vol 115, pp., 2015.

[11] S. Masuda, and E. Miura, "Generation and analysis of quasimonoenergetic electron beams by laser-plasma interaction in transitional region from the self-modulated laser wakefield to bubble acceleration regime," Phys. Plasmas,vol 16, pp., 2009.

[12] B. Hidding, "Quasimonoenergetic electron acceleration in the self-modulated laser wakefield regime," Phys. Plasmas,vol 16, pp., 2009.

[13] C. Y. Hsieh, M. W. Lin, and S. H. Chen, "Simulation study of the sub-terawatt laser wakefield acceleration operated in self-modulated regime," Phys. Plasmas, vol 25, pp., 2018.

[14] N. Lemos, "Self-modulated laser wakefield accelerators as x-ray sources," Plasma Phys. Contr. Fus.,vol 58, pp., 2016.

[15] K. Foelsch, "The Analytical Design of an Axially Symmetric Laval Nozzle for a Parallel and Uniform Jet," J. Aeronaut. Sci., vol 16, pp. 161-&, 1949.

[16] S. Lorenz, "Characterization of supersonic and subsonic gas targets for laser wakefield electron acceleration experimentsx," Matter and Radiation at Extremes,vol 4, pp., 2019.

[17] N.D.V. Junior, 'Laser particle acceleration in Brazil', in Editor (Ed.)^(Eds.): 'Book Laser particle acceleration in Brazil' (ABEN, 2019, edn.), pp. 13

[18] N. D. Vieira, R. E. Samad, and E. P. Maldonado, 'Compact Laser Accelerators Towards Medical Applications – perspectives for a Brazilian Program'. Proc. 2019 SBFoton International Optics and Photonics Conference (SBFoton IOPC), 7-9 Oct. 2019 2019 pp. Pages

[19] F. Rodriguez, "Laval nozzle flow characterization by Fourier-transform Mach-Zehnder interferometry," in Optical Measurement Systems for Industrial Inspection IV, Pts 1 and 2, Osten, W., Gorecki, C. and Novak, E. Eds. Bellingham: Spie-Int Soc Optical Engineering, 2005, pp. 865-873.

[20] R. E. Samad, A. V. F. Zuffi, E. P. Maldonado, and N. D. Vieira, 'Development and Optical Characterization of Supersonic Gas Targets for High-Intensity Laser Plasma Studies'. Proc. 2018 SBFoton International Optics and Photonics Conference (SBFoton IOPC), Campinas, Brazil 8-10 Oct. 2018 2018 pp. Pages

[21] F. Sylla, M. Veltcheva, S. Kahaly, A. Flacco, and V. Malka, "Development and characterization of very dense submillimetric gas jets for laser-plasma interaction," Rev Sci Instrum, vol 83, pp. 033507, 2012.

[22] A. K. Arunachalam, "Investigation of laser-plasma interactions at near-critical densities," University of Jena, 2017

[23] H. A. Lorentz, "Über die Beziehungzwischen der Fortpflanzungsgeschwindigkeit des Lichtes derKörperdichte," Ann. Phys. 9, 641-665, 1880.

[24] L. Lorenz, "Über die Refractionsconstante," Ann. Phys. vol 11, 70-103, 1880.

[25] T. N. Olney, N. M. Cann, G. Cooper, and C. E. Brion, "Absolute scale determination for photoabsorption spectra and the calculation of molecular properties using dipole sum rules," Chem. Phys., vol 223, pp. 59-98, 1997.

[26] L. M. Smith, D. R. Keefer, and S. I. Sudharsanan, "Abel inversion using transform techniques," Journal of Quantitative Spectroscopy and Radiative Transfer,vol 39, pp. 367-373, 1988.

[27] S. Shi, K. Finch, Y. She, and G. Gamez, "Development of Abel's Inversion Method to Extract Radially Resolved Optical Emission Maps from Spectral Data Cubes Collected via Push-Broom Hyperspectral Imaging with Sub-pixel Shifting Sampling," J. Anal. At. Spectrom., 2019.

[28] L. Rovige, "Symmetric and asymmetric shocked gas jets for laser-plasma experiments". arXiv:2103.12408, vol 1, [physics.ins-det].